Available online at www.sciencedirect.com
ScienceDirect
Ceramics International 35 (2009) 421–426
CERAMICS INTERNATIONAL
www.elsevier.com/locate/ceramint

Fabrication and characterization of $Li_{1+x-y}Nb_{1-x-3y}Ti_{x+4y}O_3$ substrates using aqueous tape casting process

Shaochun Li, Qilong Zhang, Hui Yang *, Dong Zou

Department of Materials Science and Engineering of Zhejiang University, Hangzhou 310027, China

Received 11 September 2007; received in revised form 13 October 2007; accepted 2 December 2007
Available online 8 April 2008

Abstract

An aqueous system for tape casting $Li_{1+x-y}Nb_{1-x-3y}Ti_{x+4y}O_3$ (LNT) ceramics was developed using poly(vinyl alcohol) (PVA) binder, ethylene alcohol (EG) plasticizer and ammonium salt of polycarboxylate (PCA-NH_4) dispersant. The zeta potential measurement showed that the isoelectric point of the LNT particles moved slightly toward more acid region after the dispersant absorbed on the particles, while the zeta potential increased significantly. The rheological test indicated that the ceramic slurry exhibited a typical pseudoplastic behavior without thixotropy. The effect of solid loading on the properties of the green tapes was investigated. The increase in the solid loading increased the tensile strength and the green density of the tapes. TGA analysis indicated that the organic additives in the green tapes can be completely removed by heat treatment at 600 °C. SEM micrographs showed that the microstructure of the green and sintered tapes was homogeneous.

Keywords: A. Tape casting; C. Mechanical properties; Substrates; $Li_{1+x-y}Nb_{1-x-3y}Ti_{x+4y}O_3$

1. Introduction

Tape casting was invented as a forming method for ceramics in 1947, when Howatt et al. [1] used the tape casting machine to produce ceramic capacitors. This forming method is routinely used today in the manufacture of products such as multilayer ceramic capacitors (MLCCs) [2,3], low temperature co-fired ceramic (LTCC) [4,5], lithium batteries [6] and fuel cells [7,8]. Traditionally, a variety of non-aqueous organic solvents, such as alcohols, ketones and hydrocarbons are commonly used in tape casting process.

In recent years, the environmental and health aspects of the tape casting process have received comprehensive attention. There is now a trend to move away from organic solvents and an expected transition towards water-based systems. The main advantages for switching from organic to water-based systems are reduced health and environmental hazards coupled with a lower cost. The disadvantages of using water-based systems, however, are the slower drying rate and the higher chance of cracking. In comparison with organic solvent-based tape casting slurries, aqueous tape casting systems have a smaller tolerance to minor changes in processing parameters, such as composition, and drying conditions. So far, aqueous tape casting has been successfully applied to many advanced ceramics such as Al_2O_3 [9–17], $BaTiO_3$ [18], Si_3N_4 [19,20], AlN [21,22], SiC [23], etc.

The rapid growth of the wireless communication industry has created a high demand for microwave ceramic components. Recent studies have demonstrated that the solid solution $Li_{1+x-y}Nb_{1-x-3y}Ti_{x+4y}O_3$ (LNT), also referred to as the ''M-Phase'', exhibit chemically tunable dielectric properties of interest for use in wireless communication systems. Therefore, LNT was known as potential candidate materials for LTCC application with high dielectric constant, low loss and stable temperature coefficient of resonance frequency [24–29]. So, it is important to investigate the tape casting process of LNT powders. However, to the best of our knowledge, only scant literature on LNT materials prepared by aqueous tape casting process has been reported.

In this work, we discuss the use of PVA as binder for aqueous tape casting of LNT ceramic. The rheological properties of ceramic slurry, the properties of the green tapes were studied. The microstructure of the tapes was investigated before and after sintering.

* Corresponding author. Tel.: +86 571 87951408; fax: +86 571 87953054.
E-mail address: mse237@zju.edu.cn (H. Yang).

0272-8842/$34.00.
doi:10.1016/j.ceramint.2007.12.003

2. Experimental procedure

2.1. Materials

LNT powders were synthesized by conventional mixed oxide method. Reagent-grade dried Li_2CO_3, Nb_2O_5, TiO_2 (all 99.9% purity) powders were used as starting materials. The raw materials were ball-milled in ethanol using ZrO_2 balls for 24 h. The mixture was dried and annealed at 900 °C. The XRD pattern was recorded on a Rigaku D/max-RA diffractometer using Cu Kα radiation generated at 36 kV and 30 mA. Fig. 1 illustrates the XRD analysis of the LNT powders. The XRD pattern confirms that the ceramic is composed of two phases, "M-Phase" ($Li_{1.075}Nb_{0.625}Ti_{0.45}O_3$) and Li_2TiO_3.

Poly(vinyl alcohol) (PVA 1750, 10 wt.% water solution) was selected as binder and ethylene glycol (EG) as plasticizer. The ammonium salt of polycarboxylate (PCA-NH_4) with molecular weight of 5000 g/mol was used as dispersing agent. The additives used in this paper are listed in Table 1. The amount of binder, plasticizer, and dispersant is expressed on a dry weight of the powder basis.

2.2. Zeta potential

Zeta potential of the LNT suspension was determined by Zeta-Probe Analyzer (Colloidal Dynamics Corp., USA). Suspensions were prepared by dispersing LNT particles in deionized water both in the absence and presence of the dispersant at various pH levels. The pH levels were adjusted with analytical grade HCl and NaOH.

2.3. Slurry preparation

Tape casting slurries were prepared by the following procedures. First, LNT particles (3.9 g/cm^3) were dispersed using the dispersant in deionized water with the pH value adjusted within the range of 9.0–10.0. Subsequently, the slurries were subjected to ball milling with ZrO_2 balls for 12 h. Next, the binder and plasticizer were added, and the slurries were ball-milled for another 1 h to achieve homogeneity. This procedure is shown in Fig. 2.

Table 1
Additives used in aqueous tape casting

Additives	Function	Amount (%)
PVA	Binder	5
EG	Plasticizer	10
PCA-NH_4	Dispersant	0.2

2.4. Rheology measurement

The rheological behavior of the slurries with 19.7, 25.0 and 31.9 vol.% solid loadings was characterized using a controlled stress rheometer (Haake VT550, Germany) at 25 °C shear-dependent behavior of the examined system under steady shear conditions was evaluated by ascending and descending shear rate from 0 to 400 s^{-1} in 2 min, and from 400 to 0 s^{-1} in 2 min, respectively.

2.5. Tape casting

Before casting, the slurry was first filtered using a 30 μm mesh and then de-aired under vacuum to remove any entrapped air bubbles. Tape casting was done with moving single doctor blade on glass substrate. The casting speed was constant at 1 cm/s and the gap between the blade and the carrier film adjusted at 200–300 μm. After tape casting, the tapes were left to dry at room temperature for 2 h, and then dried at 80 °C for another 15 min. Then the tapes were peeled off from the carrier.

2.6. Characterization of green tapes

Tensile testing of green tapes with different solid loadings was performed by an Instron Universal Testing Instrument (AG-1 Instron tensile tester, Japan) at a constant load speed of

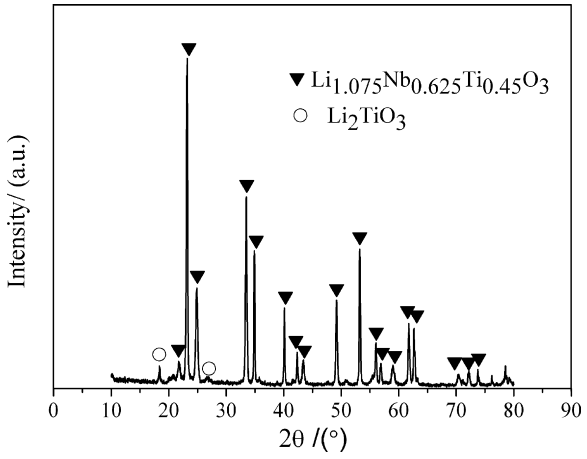

Fig. 1. XRD pattern of LNT powders.

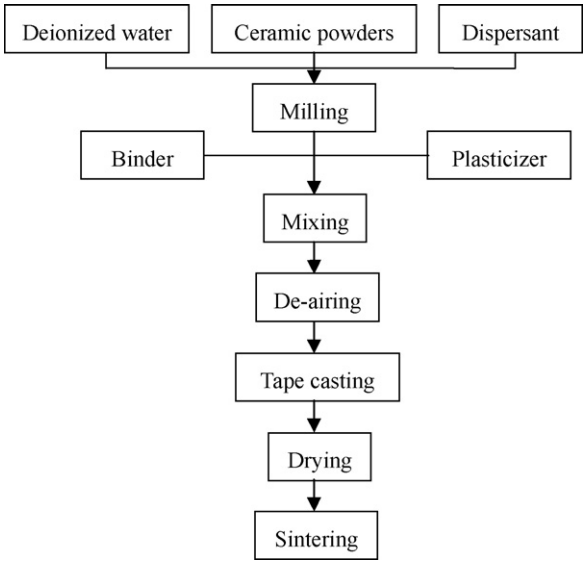

Fig. 2. The aqueous tape casting flow process chart of LNT ceramic.

2.5 mm/min. Tensile bar specimens (dog-bone shape) with 20 mm width and 50 mm gauge length were cut from green tapes using a razor blade. The stress and strain values obtained correspond to the average of at least 10 measurements.

The density and pore size distribution of the green tapes were measured by mercury porosimetry (AutoPore IV 9510, Micrometric Corp., USA).

2.7. Sintering

In order to determine the decomposition characteristics of the organic additives within the green tapes and hence the optimum heating rate for sintering, TG/DTA analysis (WRT-3P and CRY-2P, China) was performed in an air atmosphere using a heating rate of 10 °C/min. The green tapes were heated up to 600 °C at a heating rate of 1 °C/min and held 1 h to slowly burn out all organic additives. Then a heating rate of 5 °C/min was applied to achieve the final sintering temperature of 1000 °C and 1050 °C. The tapes were sintered for 2 h.

Microstructure of the both green tapes and sintered tapes was observed using a scanning electron microscopy (SEM, Hitachi S-570, Japan).

3. Results and discussion

3.1. Zeta potential

Fig. 3 shows the zeta potential of LNT ceramic particles with and without the dispersant. The isoelectric point (IEP) of LNT particles without dispersant is found at about pH 3. The absolute value of zeta potential was about 30 mV at pH 9–10 without dispersant. With the addition of dispersant, the IEP was moved to about pH 2.4. The addition of dispersant made the IEP of LNT shifted to the smaller pH value. Meantime, the absolute values of zeta potential markedly increased to 70 mV at pH 9–10. Form Fig. 3, it also can be seen that the value of zeta potential was very high at pH 2, but this value was instability at this pH range. So the pH value of the slurries was adjusted at 9–10 in this paper. The dispersion mechanism of PCA-NH_4 is based on both electrostatic repulsion and steric stabilization. Anionic polyelectrolyte can absorb on the particles surface and acquire high stabilization energy. In the meantime, the polyelectrolyte can dissociate and cause the electrostatic repulsion among particles. Therefore, the addition of PCA-NH_4 made the LNT particles produce a high surface-charged density.

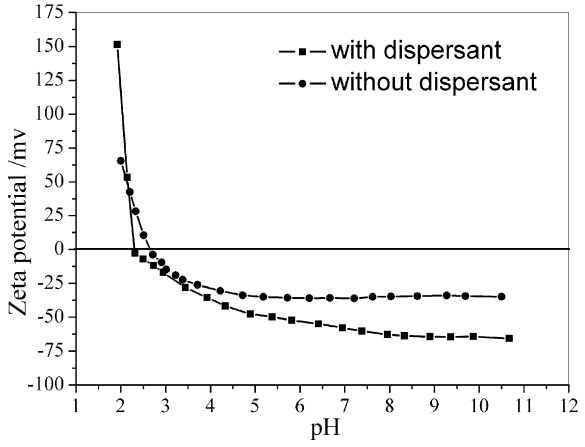

Fig. 3. The relationship between pH value and zeta potential.

3.2. Rheology property

Rheological property of the tape casting slurry was shown in Fig. 4. It can be seen from Fig. 4a that the curve for 19.7 vol.% loading exhibited characteristics close to Newtonian behavior, although a slight shear thinning was observed. The characteristic is typical of stable colloidal slurry. When the solid loading was increased to 25.0 and 31.9 vol.%, the slurries showed typical shear thinning behavior over the applied shear rate. Meanwhile, the viscosity increased with increasing solid loading. As seen in Fig. 4b, the curves for 19.7, 25.0 and 31.9 vol.% loading exhibited no time-dependent behavior since the increasing and decreasing shear rate curves coincided fairly well. The shear thinning behavior has been interpreted as a result of the gradual breaking of the structures formed while the fluid was in repose, indicating that a high shear stress is necessary to break them. At low shear rates, the slurry structure is close to equilibrium, and thermal motion dominates over viscous forces. At higher shear rates, the viscous forces affect

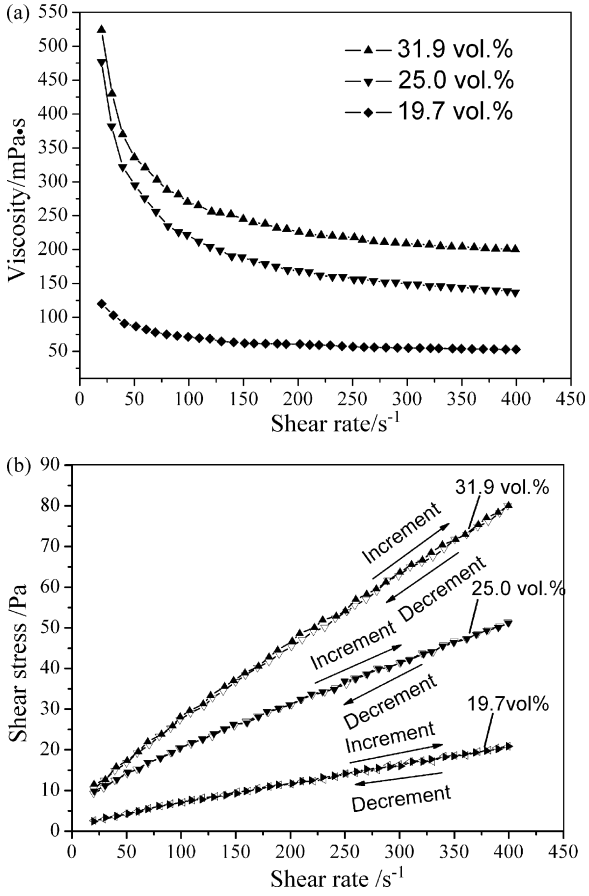

Fig. 4. Rheological curves for the slurries prepared with different LNT solid loadings (a) viscosity vs. shear rate curves and (b) shear stress vs. shear rate curves.

the slurry structure more, causing the slurry structure to become distorted, hence leading to shear thinning. The shear thinning behavior is desired for the tape casting process. In addition, a low viscosity of 280 mPa s at shear rate of 100 s^{-1} was observed from Fig. 4a, thus confirming the good dispersing ability of the PCA-NH_4 for LNT aqueous slurries, even for high solid loading.

3.3. Characterization of green tapes

Fig. 5 shows typical tensile curves for the green tapes prepared with 19.7, 25.0 and 31.9 vol.% of LNT solid loading. It can be seen that all tapes exhibited well ductile behavior and the ductile behavior became more noticeable with a decrease of the solid loading. As a general trend, the maximum stress increases and the maximum strain decreases with increasing solid loading. For 31.9 vol.% solid loading, the maximum stress reached 1.73 MPa and the strain to failure was about 24% of the initial probe size, compared with 1.26 MPa and 45% in case of 19.7 vol.% solid loading, respectively. This result illustrated that water is another effective plasticizer for PVA binder. So, its necessary to maintain a residual humidity in the tapes.

Fig. 6 shows pore size distributions of the green tapes derived from slurries containing different solid loadings. All samples had a similar narrow micropore size distribution with pore radius between 0.009 and 1.0 μm and the most frequent pore radius was 0.055 μm. However, the porosity of the tapes was different. The porosity gradually decreased with increasing solid loading and thereby with increasing the green density. This reduction of the porosity produced the increase in the green density of the tapes. Table 2 shows the porosity and the green density of the tapes with different solid loadings. The sample containing 19.7 vol.% loading exhibited the highest porosity. The difference between porosities of the tapes with 19.7 vol.% (53.3%) and 25.0 vol.% (52.8%) loading was small. As solid loading increased to 31.9 vol.%, the influence of solid loading on the porosity became more significant, in which the porosity was 48.7%.

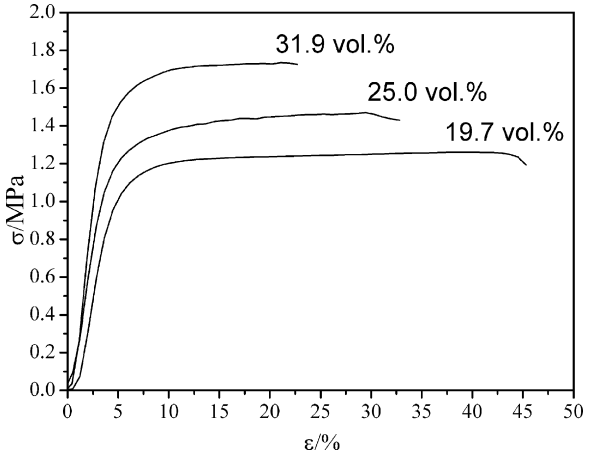

Fig. 5. Stress–strain curves for green tapes prepared with different LNT solid loadings.

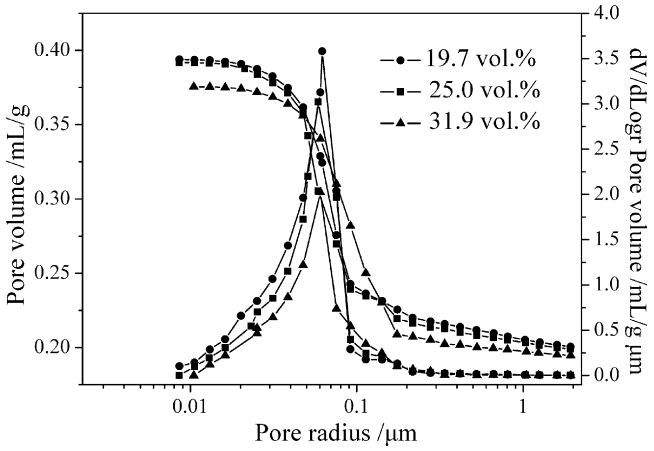

Fig. 6. Pore size distribution of the green tapes with different solids loadings.

3.4. Microstructure of the green tapes

The microstructural evolution of the green tapes with increasing solid loading as observed by SEM is shown in Fig. 7. Generally, the tapes showed a smooth and well-packed surface morphology with average particle size between 1 and 2 μm. As expected, the pore size distribution decreased with increasing solid loading. The tapes derived from the slurry containing 19.7 and 25.0 vol.% loading have a heterogeneous microstructure with large pores, in which LNT particles do not completely occupy all the voids. As solid loading gradually increased to 31.9 vol.%, the microstructure of the green tape became more homogeneous and denser. These observations coincide with the porosity measurements very well.

3.5. TG/DTA analysis

Thermal analysis of the green tapes has been performed by combined TG/DTA measurement. The results are presented in Fig. 8. The endothermic curve descending around 80–230 °C corresponding to the weight loss was owing to the volatilization of the water. The exothermic curve around 230–340 °C, accompanied by sharp weight loss, was due to the decomposition of the organic additives. The endothermic curve descending around 340–500 °C corresponding to the weight loss was associated with the carbonization of the organic additives. The TG curve showed that there was no obvious weight change when the temperature was higher than 600 °C, and the corresponding slow ascending exothermic curve in DTA was due to the gradual combustion of the residue carbon.

Table 2
The porosity and the green density of the tapes with different solid loadings

Item	Solids loading		
	19.7 vol.%	25.0 vol.%	31.9 vol.%
Porosity (%)	53.3	52.8	48.7
Green density (g/cm^3)	1.82	1.84	2.00

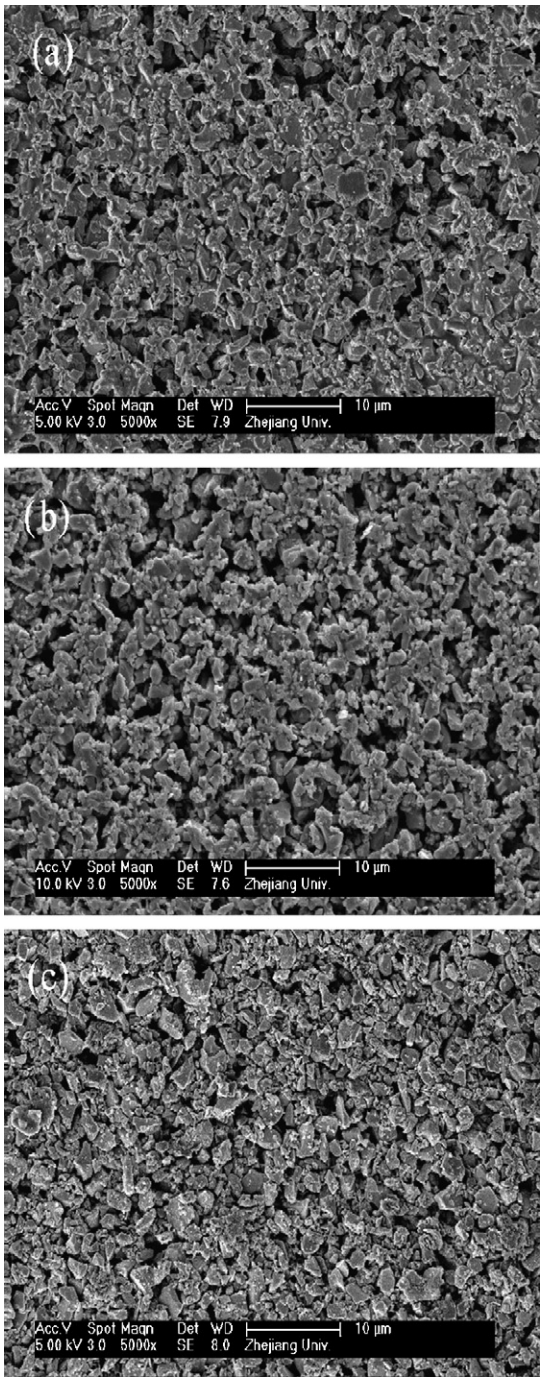

Fig. 7. SEM of green tapes with different solid loadings: (a) 19.7 vol.%; (b) 25.0 vol.%; (c) 31.9 vol.%.

3.6. Microstructure of the sintered tapes

The SEM micrographs of the tapes with solid loading of 31.9 vol.% sintered at 1000 and 1050 °C are shown in Fig. 9. The relative density of the tapes sintered at 1000 and 1050 °C is 92% and 95%, respectively. From Fig. 9a, long-platelet shaped grains with thickness of 1–2 μm and diameter of 6–10 μm could be observed. After sintering at 1000 °C, samples show high residual porosity and was not dense. With the sintering temperature increased, the sample was

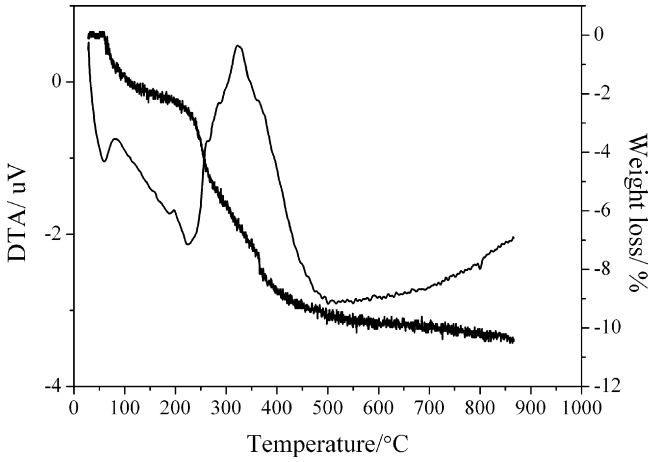

Fig. 8. TG/DTA plot of the green tape.

fully dense with fairly uniform microstructure, but due to shorter sintering time, a few pores existed in the sample (Fig. 9b). However, the grain size in Fig. 9b seems smaller than that in Fig. 9a, although the sample has been sintered at a higher temperature (1050 °C). This phenomenon was unable to explain and needs further study.

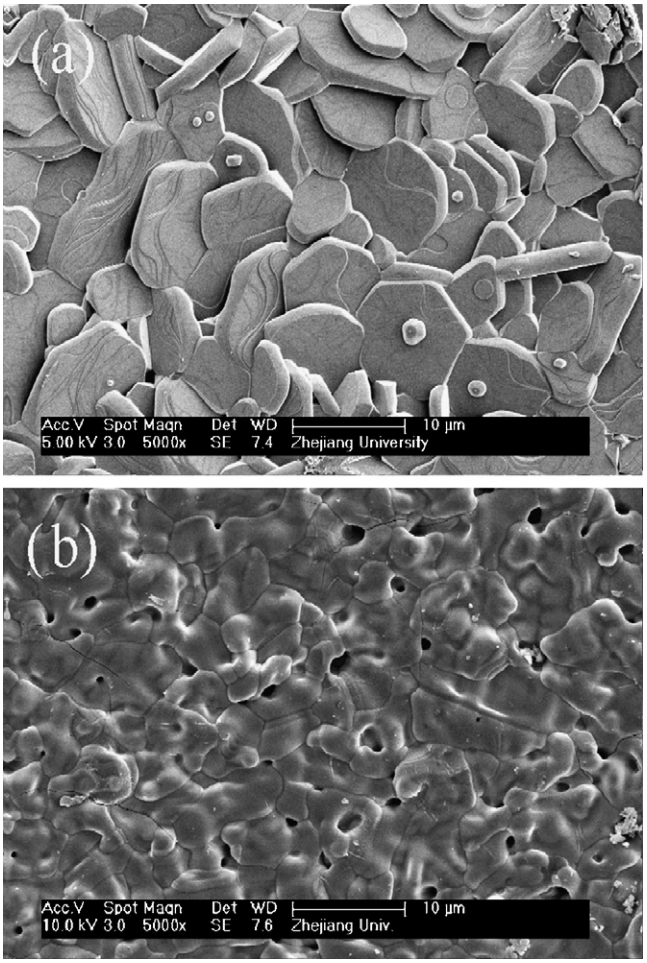

Fig. 9. SEM of the tapes with solid loading of 31.9 vol.% sintered at different temperatures: (a) 1000 °C; (b) 1050 °C.

4. Conclusions

Aqueous tape casting of LNT ceramic was successfully performed by using PVA binder, EG plasticizer, and PCA-NH_4 dispersant. In the presence of PCA-NH_4 dispersant, the IEP of LNT powders shifted from pH 3.0 to 2.4 and the absolute value of zeta potential increased from 30 to 70 mV at pH 9–10, this was attributed to charge reversal as PCA-NH_4 was absorbed on the LNT surface. The rheological properties, especially the degree of pseudoplasticity and the viscosity, increased significantly with solid loading. The mechanical property measurements showed that the tensile strength increased and the strain-to-failure decreased with increasing solid loading. Furthermore, it was found that the porosity of the green tapes decreased from 53.3% to 48.7% when the solid loading increased from 19.7 to 31.9 vol.%. In conclusion, LNT sheets with well flexibility and homogeneous microstructure could be prepared using an aqueous tape casting technique.

Acknowledgement

This study was supported by the Key Scientific and Technological Project of Zhejiang Province (2006C21071).

References

[1] G.N. Howatt, R.G. Breckenridge, J.M. Brownlow, Fabrication of thin ceramic sheets for capacitors, J. Am. Ceram. Soc. 30 (1947) 237–242.
[2] D.H. Yoon, B.I. Lee, Processing of barium titanate tapes with different binders for MLCC applications. Part I: Optimization using design of experiments, J. Eur. Ceram. Soc. 24 (2004) 739–752.
[3] D.H. Yoon, B.I. Lee, Processing of barium titanate tapes with different binders for MLCC applications. Part II: Comparison of the properties, J. Eur. Ceram. Soc. 24 (2004) 753–761.
[4] H. Jantunen, T. Hu, A. Unsimaki, S. Leppavuori, Tape casting of ferroelectric, dielectric, piezoelectric and ferromagnetic materials, J. Eur. Ceram. Soc. 24 (2004) 1077–1081.
[5] Q.X. Zhang, X.J. Luo, W.L. Li, H.R. Zhuang, D.S. Yan, Tape casting of AlN/glass composites for LTCC substrate, J. Mater. Sci. 38 (8) (2003) 1781–1785.
[6] J.-H. Lee, U. Paik, A.H. Vincent, Y.-H. Choi, Effect of poly(acrylic acid) on adhesion strength and electrochemical performance of natural graphite negative electrode for lithium-ion batteries, J. Power Sources 161 (2006) 612–616.
[7] S. Beaudet Savignat, M. Chiron, C. Barthet, Tape casting of new electrolyte and anode materials for SOFCs operated at intermediate temperature, J. Eur. Ceram. Soc. 27 (2007) 673–678.
[8] L.H. Luo, A.I.Y. Tok, F.Y.C. Boey, Aqueous tape casting of 10 mol%-Gs_2O_3-doped CeO_2 nano-particles, Mater. Sci. Eng. A 429 (2006) 266–271.
[9] C. Pagnoux, T. Chartier, M. de, F. Granja, F. Doreau, J.M. Ferreira, L.F. Baumard, Aqueous suspensions for tape-casting based on acrylic binders, J. Eur. Ceram. Soc. 18 (1998) 241–247.
[10] A. Kristoffersson, E. Carlström, Tape casting of alumina in water with an acrylic latex binder, J. Eur. Ceram. Soc. 17 (1997) 289–297.
[11] F. Doreau, G. Tarì, C. Pagnoux, T. Chartier, J.M. Ferreira, Processing of aqueous tape-casting of alumina with acrylic emulsion binders, J. Eur. Ceram. Soc. 18 (1998) 311–321.
[12] R. Greenwood, E. Roncari, C. Galassi, Preparation of concentrated aqueous alumina suspensions for tape casting, J. Eur. Ceram. Soc. 17 (1997) 1393–1401.
[13] C.A. Gutiérrez, R. Moreno, Influence of slip preparation and casting conditions on aqueous tape casting of Al_2O_3, Mater. Res. Bull. 36 (2001) 2059–2072.
[14] X.M. Cui, S.X. Ouyang, Z.Y. Yu, C.A. Wang, Y. Huang, A study on green tapes for LOM with water-based tape casting processing, Mater. Lett. 57 (2003) 1300–1304.
[15] Y.H. Zhang, C.W. Qin, J. Binner, Processing multi-channel alumina membranes by tape casting latex-based suspensions, Ceram. Int. 32 (2006) 811–818.
[16] M.P. Albano, L.B. Garrido, Influence of the slip composition on the properties of tape-cast alumina substrates, Ceram. Int. 31 (2005) 57–66.
[17] Y.P. Zeng, D.L. Jiang, P. Greil, Tape casting of aqueous Al_2O_3 slurries, J. Eur. Ceram. Soc. 20 (2000) 1691–1697.
[18] Y.L. Song, X.L. Liu, J.Q. Zhang, X.Y. Zou, J.F. Chen, Rheological properties of nanosized barium titanate prepared by HGRP for aqueous tape casting, Powder Technol. 155 (2005) 26–32.
[19] B. Bitterlich, J.G. Heinrich, Aqueous tape casting of silicon nitride, J. Eur. Ceram. Soc. 22 (2002) 2427–2434.
[20] J.X. Zhang, F. Ye, D.L. Jiang, M. Iwasa, Preparation of bulk Si_3N_4 from tape casting and lamination, Ceram. Int. 32 (2006) 277–282.
[21] S.M. Olhero, J.M.F. Ferreira, Rheological characterization of water-based AlN slurries for the tape casting process, J. Mater. Process. Technol. 169 (2005) 206–213.
[22] X.J. Luo, B.L. Zhang, W.L. Li, H.R. Zhuang, Preparation of aluminum nitride green sheets by aqueous tape casting, Ceram. Int. 30 (2004) 2099–2103.
[23] J.X. Zhang, R. Huang, H. Gu, D.L. Jiang, Q.L. Lin, Z.R. Huang, High toughness in laminated SiC ceramics from aqueous tape casting, Scripta Mater. 52 (2005) 381–385.
[24] A. Borisevich, P.K. Davies, Microwave dielectric properties of $Li_{1+x-y}M_{1-x-3y}Ti_{x+4y}O_3$ ($M = Nb^{5+}$, Ta^{5+}) solid solutions, J. Eur. Ceram. Soc. 21 (2001) 1719–1722.
[25] Q.L. Zhang, H. Yang, X.Y. Liu, D.L. Lu, $Li_{1.05}Nb_{0.55}Ti_{0.55}O_3$ microwave dielectric ceramics prepared by low-temperature sintering and their microwave device, J. Chin. Ceram. Soc. 33 (2005) 793–798.
[26] L. Farber, I. Levin, A. Borisevich, I.E. Grey, R.S. Roth, P.K. Davies, Structural study of $Li_{1+x-y}Nb_{1-x-3y}Ti_{x+4y}O_3$ solid solutions, J. Solid State Chem. 166 (2002) 81–90.
[27] D.H. Kang, K.C. Nam, H.J. Cha, Effect of Li_2O–V_2O_5 on the low temperature sintering and microwave dielectric properties of $Li_{1.0}Nb_{0.6}$-$Ti_{0.5}O_3$ ceramics, J. Eur. Ceram. Soc. 26 (2006) 2117–2121.
[28] Q. Zeng, W. Li, J.L. Shi, J.K. Guo, Microwave dielectric properties of $5Li_2O$–$0.583Nb_2O_5$–-3.248TiO_2 ceramics with V_2O_5, J. Am. Ceram. Soc. 89 (2006) 261–265.
[29] X.Y. Liu, Q.L. Zhang, H. Yang, J.X. Tong, D.L. Lu, The influence of different introduce mode of V_2O_5 on the microwave dielectric properties of Li_2O–Nb_2O_5–TiO_2, Electron. Comp. Mater. 23 (2004) 15–18.